17th Australasian Fluid Mechanics Conference
Auckland, New Zealand
5-9, December, 2010

New drag balance facility for skin-friction studies in turbulent boundary layer at high Reynolds numbers

Krishna T. M., C. M. de Silva and I. Marusic

Department of Mechanical Engineering
The University of Melbourne, Victoria, 3010, AUSTRALIA

Abstract

A unique drag balance facility is described here for the study of skin-friction in high Reynolds number wall turbulence. The facility was tested in the High Reynolds Number Boundary Layer Wind Tunnel (HRNBLWT) at the University of Melbourne, giving direct measurements of skin-friction over a large surface. The approach utilizes a drag balance, however, here the implementation is unique in two aspects, the design and the Reynolds number at which the experiments were conducted. The drag balance consists of a large floating flat plate whose displacement is translated into a force measurement by a load cell. Measurements of skin-friction coefficient c_f at different Reynolds numbers were obtained, and are compared with those obtained using a Clauser-chart method. Comparisons are also made with various empirical relations for c_f available in literature. Both comparisons showed a very good collapse, which establishes the utility of the facility in determining wall shear stress.

Introduction

Wall-shear stress, or skin-friction, is the local tangential force per unit area exerted on a body as a result of fluid flow over it. The shear stress is manifested through the boundary layer which exists as a consequence of the no-slip condition at the wall and is the region of high shear between the wall and the outer free-stream flow. The practical importance of wall turbulence has made it an active area of research for the past 100 years as to a great extent, the behaviour of turbulent boundary layer determines the performance of many aerodynamic surfaces (e.g., wings, propellers and fans). Of fundamental importance to this problem is the need to understand the behaviour of the wall-shear stress, denoted by τ_w. The accurate

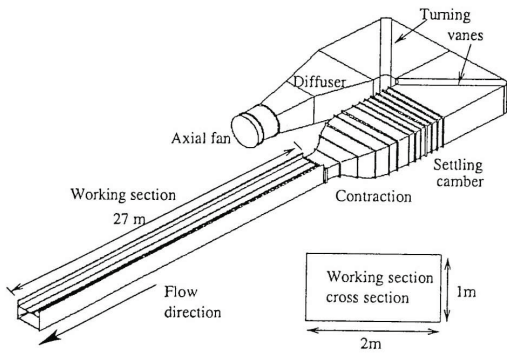

Figure 1: Schematic of wind tunnel (HRNBLWT) used in the experiment

measurement of τ_w has long been a challenge. It has classically been derived by integrating the momentum equation along with the appropriate mean velocity profile across the boundary layer. Most indirect techniques, that have been used so far suffer from limitation in their applicability. The most prominent method used is the Clauser-chart [1], wherein, c_f is obtained

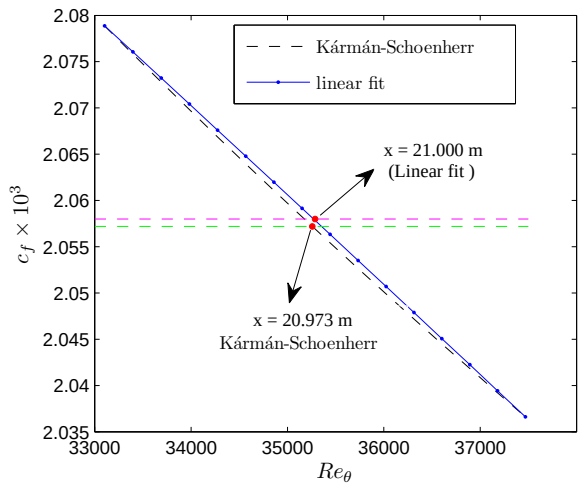

Figure 2: Comparison of c_f obtained using Kármán-Schoenherr fit and linear fit, in Re_θ range obtained over the length of drag plate at the free stream velocity of U_∞ = 20 m/s

by fitting the logarithmic velocity profile to the measured mean velocity [4]. It inherently assumes the existence of a universal law of the wall *i.e.* logarithmic profile for the mean velocity but the indication from other indirect measurements of u_τ, was that the constants that describe the logarithmic profile differed from their accepted values [7]. The next commonly used method involves using the Kármán integral momentum equation [6] by calculating the development of momentum thickness downstream based on the relation $c_f \simeq d\theta/dx$. This needs very detailed stream-wise development measurements and differentiation of experimental data which is prone to errors. In addition, this method is sensitive to weak pressure gradients and residual three-dimensionality that exist in nominally two-dimensional, zero-pressure gradient test sections, and potentially lead to inaccurate results [12]. The third method of obtaining c_f is to find the mean velocity gradient close to the wall, $\tau = \mu(dU/dy)_{y\to 0}$ [4]. This method suffers from the difficulty in making measurements very close to the wall, with conduction and blockage issues for hot-wires and correction schemes required for Pitot tubes.

On the other hand, wall shear stress can also be determined independent of the velocity profile. A floating element and an oil-film interferometry technique are the primary means of achieving this [13]. Recent advances enable us to obtain more accurate results using these methods [11]. These include extensive experimental analysis on floating element devices by Osaka *et. al.* [9] to measure local skin-friction resistance in a zero-pressure gradient boundary layer and the work by Nagib *et. al.* [6] and Osterlund *et. al.* [10] in improving the oil film technique.

Many previous studies with a floating-plate drag balance as re-

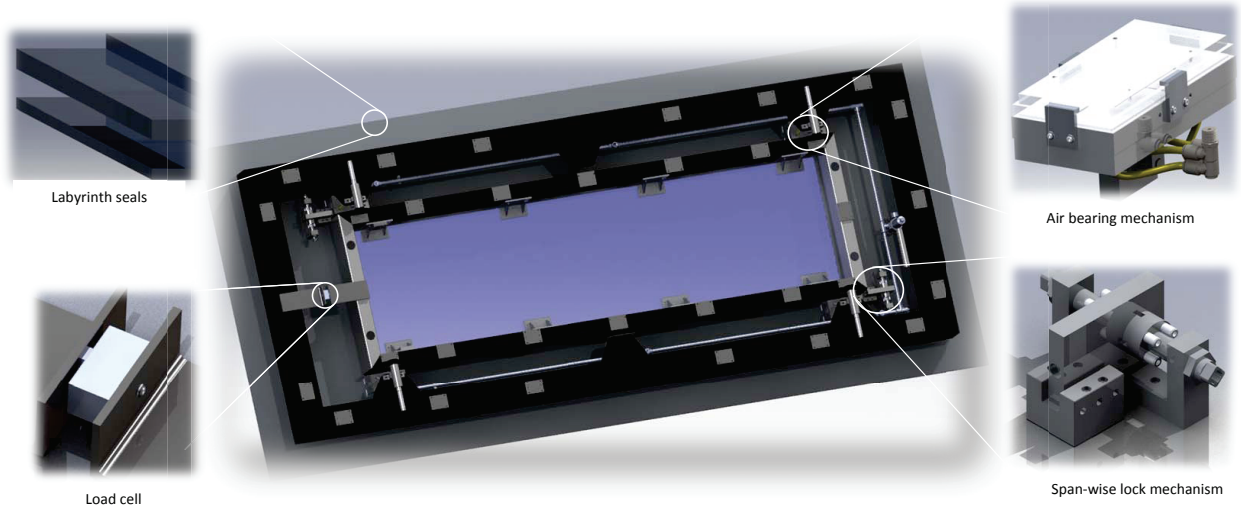

Figure 3: Three dimensional CAD model of drag balance, with all the individual components.

ported by Savill *et al.* [12] rely on local skin-friction c_f measurements. The problem with these measurements is that they do not account for the parasitic drag or any other additional form drag associated with the design. One of the problems most small wind tunnel facilities face is the small viscous length scale ν/U_τ at high Reynolds number measurements. This problem is reduced in the present large-scale facility (HRNBLWT), a schematic of which is shown in figure 1. This facility is especially designed for the experimental study of high Reynolds number boundary layers with sufficient thickness to provide good spatial resolution. The working section of the HRNBLWT has a cross section of 2m width and 1m height, and is 27m in length. The long working section allows the boundary layer to grow over a long distance, thereby producing a high Reynolds number, with a thick boundary layer. The boundary layer near the working section of the drag balance is approximately 350mm thick and is 20m downstream from the trip, this provides a very good spatial resolution for measurements [8]. Most small facilities also face additional limitations due to alignment, gaps and leaks. To obtain large values of ν/U_τ in these, the tunnel has to be operated at low speeds giving a very low U_τ signal and thus are faced with small signals that are comparable in magnitude to noise. Due to large surface area of the drag balance facility, the average shear stress signal, which otherwise, a small signal typically ~ 0.05Pa [2], is amplified to a signal which has a bigger signal to noise ratio, thereby simplifying the analysis of drag force.

The original motivation of this facility was mainly to carry out drag reduction studies and measure the change in τ_w, *i.e.* $\Delta\tau_w$. It was designed to contain within itself all measuring instruments, the control circuitry to conduct real-time drag minimisation strategies and an on-board power source. However, due to its design we can also use the same facility to measure τ_w over a large surface. This is justified by the fact that the variation of skin-friction coefficient c_f over the length of the drag plate is approximately linear over the working section, and hence the average signal of c_f can be measured and compared to those obtained at the centre position of the drag plate. This is confirmed in figure 2 where the average c_f has been calculated using the Kármán-Schoenherr relation [6] and is compared to a linear approximation across the drag plate. The corresponding streamwise positions were then obtained for both equations. With a linear fit, the x position is obtained as 21.000m while using the Kármán-Schoenherr equation, it is found to be 20.973m, which corresponds to a negligible difference in c_f. This allows us to compare the experimental data with measurements conducted at 21m by Hutchins *et. al.*[3]. Details of the drag balance design, components and measurements at HRNBLWT are presented in the remainder of this paper.

Drag Balance

The drag balance is a large flat plate of dimensions 3m$\times$1m, mounted between streamwise positions 19.5m and 22.5m of the tunnel floor. The outer section of the drag plate is made of aluminum and the support structure is made from steel. The facility has an interchangeable central section, of either glass (providing optical access) or an aluminum plate to accommodate various experiments. The plate freely floats with the aid of four air bearings, a labyrinth seal and the span-wise locking system. Figure 3 shows a three dimensional CAD model of the entire assembly highlighting key components. The air bearing mechanism is pneumatically driven at a pressure of 80 psi. This creates a very thin layer of air [$O(\mu$m)] between the glass pads and the supporting surface of the drag plate that is mounted to the floor of the tunnel. This mechanism supports the weight of the plate and also makes it virtually frictionless, however, to ensure the mechanism works effectively, the drag plate was adjusted to remain horizontal with reference to highly sensitive spirit levels. This ensures that the weight of the drag plate itself does not contribute to the force measurement. The circumference of the drag plate consists of a gap which separates it from the rest of the floor of the tunnel. It is essential for the drag balance to perform accurately that no air escapes from this gap and there is no sudden step change in the tunnel floor as it would cause a pressure drop, typically any unevenness needs to within $3\nu/U_\tau$. However, due to the large size of the drag plate and a boundary layer thickness of approximately 350mm this facility is less susceptible to these drawbacks with previous drag balance designs. Additionally to be certain that no air can escape a labyrinth seal which is shown in figure 3 is present around the circumference of the drag plate, while still ensuring no contact

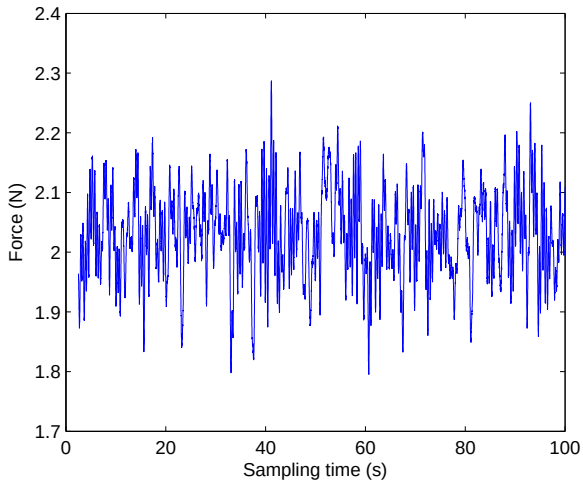

Figure 4: Typical unfiltered force signal from the transducer over a period of 60 seconds for $U_\infty \simeq 20$ m/s

between the drag plate and the tunnel floor. The third component of the assembly is the span-wise locking system, which is also pneumatically driven providing a thin layer of air between the circular pads and the vertical rectangular slab shown in figure 3. This prevents the plate from moving in the span-wise direction while still facilitating stream-wise displacement. The fourth component is a high resolution load cell that measures very small forces [$O(20\ m\text{N})$], it is mounted to one end of the drag balance as shown in figure 3.

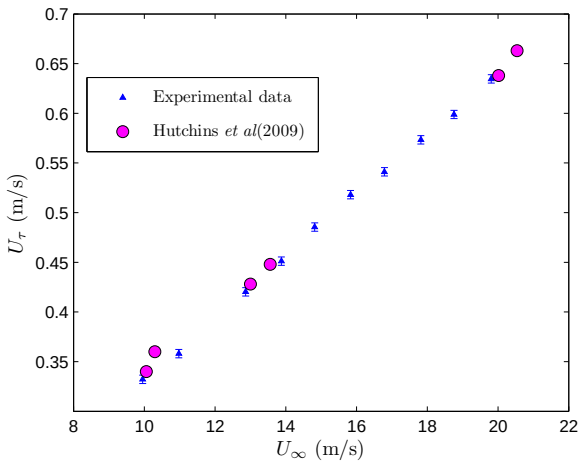

Figure 5: Comparison of U_τ with U_∞ from the drag-balance with Clauser chart results of Hutchins *et. al.* [3]

Results and Discussion

The experiments were carried out at zero-pressure gradient (ZPG) in the HRNBLWT, located in the Walter Basset Aerodynamics Laboratory at the University of Melbourne. The free stream velocity U_∞, determined by a Pitot-static tube, was varied from 10m/s to 20m/s, yielding a Reynolds number range of $Re_X = 1.4 - 2.8 \times 10^7$. The experiment had two objectives: firstly to determine how the drag balance would function in the tunnel, and secondly to investigate and compare the average wall shear stress with prior results obtained by Hutchins *et. al.* [3] for similar Reynolds numbers in the HRNBLWT and other empirical equations given in the literature [6].

Data was collected at each speed in two steps: initial pre-load on the force transducer with no-flow conditions, followed by force measurement with flow over the plate. Figure 4 shows a typical unfiltered signal from the force transducer during a sampling time of 60 seconds. In each of the stages, measurements were taken for a duration of over 180 sec and the mean was calculated. The drag force on the plate was obtained as the difference of the two values from which τ_w can be calculated. τ_w can be used to determine c_f and U_τ using equations (1) and (2) respectively.

$$c_f = \frac{\tau_w}{\frac{1}{2}\rho U_\infty^2} \tag{1}$$

$$U_\tau = \sqrt{\frac{\tau_w}{\rho}} \tag{2}$$

To establish the reliability of the measurements from the drag balance facility, experiments were conducted several times and the averaged data with error limits, is compared with those as reported by Hutchins *et. al.* [3]. Results are shown in figure 5 and table 1, it can be seen that the experimental results closely match with previous findings with a maximum percentage difference of approximately 0.95%. Hutchins *et al.* obtained U_τ using Clauser chart method where logarithmic law constants of $\kappa = 0.41$ and A = 5.0 were used. The skin-friction coefficient c_f, obtained from the drag measurements data is also plotted against Re_θ in figure 6. These are compared with the empirical relations for c_f mentioned in Nagib *et. al.* [6]. Reynolds number is calculated using equation (3), where x is the stream-wise distance from the trip to the centre of the drag plate. Re_θ is obtained from Re_X by the relationship given in equation (4), from Nagib *et. al.* [6].

$$Re_X = \frac{U_\infty x}{\nu} \tag{3}$$

$$Re_\theta = 0.01277 Re_X^{0.8659} \tag{4}$$

Conclusion

A new drag plate was tested that has the capability to measure relatively high mean values of wall-shear stress fluctuations in a turbulent boundary layer in the HRNBLWT at the University of Melbourne. The system achieved the desired force measurements at various speeds and was able to continuously measure the mean wall shear stress over a sampling period of five minutes without any drift in the measurements. The results were found to be in concurrence to the previous laboratory results conducted by Hutchins *et. al.* [3] at HRNBLWT. This suggests that the drag balance can be used with great reliability to obtain direct measurements of wall shear-stress. It also provides a greater scope for conducting various other skin-friction reduction studies on this facility.

References

[1] Clauser, F. H., Turbulent boundary layers in adverse pressure gradients, *J. Aero. Sci.*, **21**, 1954, 91-108.

[2] Heuer, W. D. C. and Marusic, I., Turbulence wall-shear stress sensor for the atmospheric surface layer, *Meas. Sci. Tech.*, **16**, 2005, 1644-1649.

[3] Hutchins, N., Nickels, T. B., Marusic, I. and Chong, M. S., Hot-wire spatial resolution issues in wall-bounded turbulence, *J. Fluid Mech.*, **635**, 2009, 103-136.

U_∞ (m/s)	U_τ (Hutchins *et al.*[3]) (m/s)	U_τ (Drag Balance) (m/s)	Absolute % difference -
10.06	0.3398	0.3422	0.68
13.00	0.4277	0.4237	0.95
20.02	0.6376	0.6383	0.10

Table 1: Comparison of U_τ data with Hutchins *et. al.* [3]

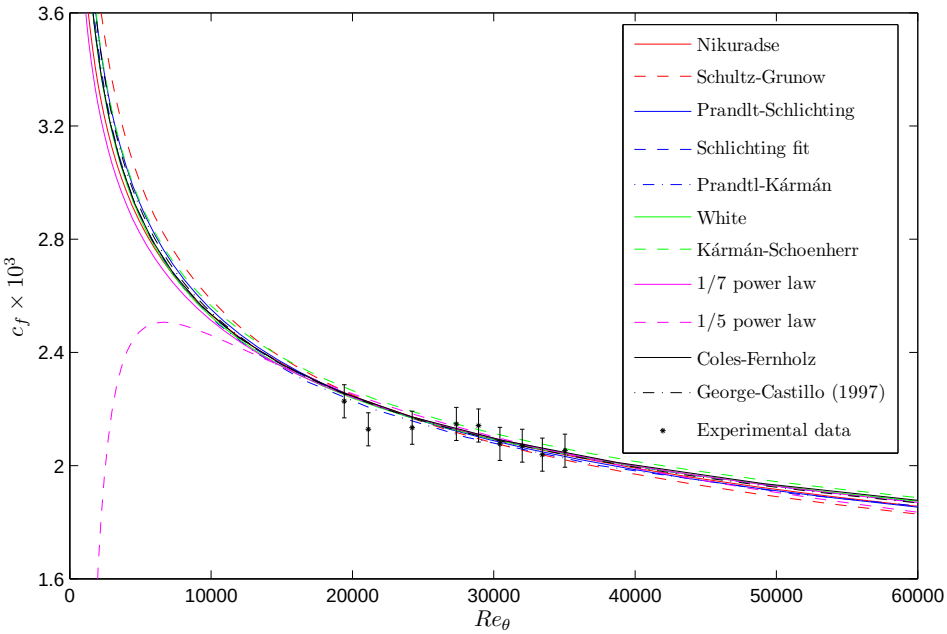

Figure 6: Comparison of c_f values with established empirical relations for c_f with Re_θ [6]

[4] Kiyoto Mori *et al*, Direct total skin-friction measurement of a flat plate in zero pressure gradient boundary layers, *Fluid Dyn. Res.*, **41**,2009.

[5] Marusic, I. and Heuer, W. D. C., Reynolds Number Invariance of the Structure Inclination Angle in Wall Turbulence, *Phys. Rev. Lett.*, **99**, 2007, 114504.

[6] Nagib, H. M., Chauhan, K. A. and Monkewitz, P. A., Approach to an asymptotic state for zero pressure gradient turbulent boundary layers, *Phil. Trans. R. Soc. A*, **365**, 2007, 755-770.

[7] Nagib, H. M. and Chauhan, K. A., Variations of von Kármán coefficient in canonical flows, *Phys.Fluids.*, **365**, 2007, 755-770.

[8] Nickels, T.B., Marusic, I., Hafez, S. and Chong, M. S., Evidence of the k_1^{-1} law in a high Reynolds number turbulent boundary layer, *Phys. Rev. Lett.*, **95**, 2005, 074501.

[9] Osaka, H., Kameda, T. and Mochizuki, S., Local skin friction coefficient evaluated by direct-measurement method and mean flow quantities in a turbulent boundary layer *JSME Int. J. Fluids Thermal Eng.Series* B, 1996, 138-45.

[10] Osterlund, J. M., Joansson, A. V., Nagib, H. M. and Hites, M. H., A note on the overlap region in turbulent boundary layers, *Phys. Fluids.*, **12**, 2000, 1-4.

[11] Ruedi, J. D., Nagib, H.M., Osterlund, J. M., and Monkewitz, P. A., Evaluation of three techniques for wall-shear measurements in three dimensional flows, *Exp. in Fluids.*, **35**, 2003, 389-396.

[12] Savill, A. M. and Mumford, J. C., Manipulation of turbulent boundary layers by outer-layer devices: skin-friction and flow-visualization, *J. Fluid Mech.*, **191**, 1988, 389-418.

[13] Winter, K. G., An outline of the techniques available for the measurement of skin friction in turbulent boundary layers, *Prog. Aero. Sci.*, **18**, 1977, 1-57.